PERFORMANCE ANALYSIS OF A VARIABLE SPEED COMPACT GSHP WITH DESUPERHEATER

David Blanco Ph.D. Candidate, Hokkaido University, Sapporo, Japan
Katsunori Nagano, Professor, Hokkaido University, Sapporo Japan

Abstract: When thinking on the thermal energetic demand for low energy houses, two heat pumps have been traditionally used: one for heating and cooling and the second one for domestic hot water. During the last two decades these two functions have been combined by attaching a desuperheater to the single frequency GSHP originally meant for space heating. Nevertheless, a variable speed GSHP can cope better with partial heat demand providing lower overall energetic consumption with no need of extra backup systems and buffer tanks which are both thermal and economically expensive. In this study, a prototype GSHP with desuperheater is examined. In order to determine an operation strategy aiming to increase the yearly performance factor, a refrigeration cycle simulation is developed, which takes into account detailed thermodynamic information as well as geometrical features of each of the components.

Key Words: Desuperheater, Refrigeration cycle Simulation, Sequential Method

1 INTRODUCTION

The year 2001 saw the commercialization for the first time of the Air source CO_2 heat pump starting a revolution in the production of domestic hot water. But the continental climate present in the north of Japan and other parts of the globe makes the seasonal performance factor of these heat pumps to be lower than their GSHP (ground source heat pumps) counterparts (Swardt and Meyer 2001). For these adverse environmental conditions, the compa ct GSHP with desuperheater can provide the thermal requirements of a low energy house in a single machine, with high efficiency and stable output.

With the purpose of examining the performance and benefits of such heat pump matching northern Japan conditions, a simulation program which can incorporate physical parameters of the elements as well as detailed thermodynamic characteristics of the system was developed. The simulation program uses convergence of mass flow rate between the compressor and the expansion valve to obtain the primary side and secondary side pressures. A Sequential module method is used to solve each of the components of the cycle. Carefully crafted initial guesses and algorithms provide lower simulation times, and minimization techniques are used for completeness. The cycle final answer is obtained by balancing the refrigerant mass charge on the system.

In order to compare the results from the simulation, a prototype GSHP with desuperheater is built and tested. Mapping results shows the limitations and advantages of the steady state operation of the machine. The simulation agrees with the experimental results within 10% for all the devices except the condenser.

2 SIMULATION

Due to the complexity of the refrigeration processes, the approach to develop refrigeration cycle models traditionally has been to conduct extended experiments on a unit and extract

performance correlations based on them (Katsura, et al. 2008) However, this approach limits the true versatility of the simulation tool as these correlations provide small applicability when the parameters of the system want to be modified; therefore while they can be good for explaining the use of a specific machine, they fail when we want to improve the current performance by a new design.

As the parameters in the refrigeration cycle are closely coupled, to find the cycle simulation solution requires of iterative and carefully crafted algorithms. Two main approaches have been traditionally used (Ding 2007): The Simultaneous Solving Method in which Newton-Raphson, Runge-Kutta or other simultaneous algorithms are applied to solve the predefined nonlinear system of equations; and the Sequential Module method, in which each of the elements of the system are solved one by one, and one or several balance conditions are used to find convergence among the variables. Although the first method is definitely faster, a solution might be obtained only if the limits of variables are carefully selected and one initial set of guesses which ideally should be very close to real solution. It is said "might find a solution" because success is not guaranteed even with the best conditions mentioned before. Finding these initial guesses to the problem might be difficult for each environmental condition that wants to be tested. On the other hand, the second approach while slower can guarantee success for every case tested. As a result, the second method is selected.

2.1 Restrictions and Assumptions

The following assumptions are taken for the development of the model:

- As the temperature outlet of the ground changes slowly throughout the year, steady state analysis is used which simplifies enormously the computational effort without losing precision on the studied physical phenomena.
- Zero pressure drops in the condensation and evaporation processes is assumed. While this can be prohibiting from the physical point of view, it greatly reduce computational requirements. Modern heat exchangers are design so as to lessen these pressure drops to a minimum; therefore in some cases it can be negligible. Some precision is inevitably lost by this assumption, though.
- While the thermodynamic properties of the refrigerant are constantly varying in the phase change process, dividing the heat exchanger into geometrical control volumes and analyzing each one becomes time consuming when we want to calculate hundreds of conditions. Therefore, the heat exchangers use the Zone model in which each zone (gas, mix or liquid) is modeled as a lumped parameter. It is found that the difference between the zone model and the distributed one is little while increasing computational speeds (Ding 2007).
- It is assumed that complete evaporation occurs in the evaporator. While at first sight this assumption might limit the model, the ground volumetric flow rates used in real installations are defined precisely to achieve this purpose, so no liquid refrigerant enters the compressor which would be fatal for the system.
- Additionally it is assumed that the pressure change inside the expansion valve follows an isenthalpic process, and no change of enthalpy between the input and output is considered.

2.2 General Model

The mass flow rate of the whole refrigeration cycle is a unique property which is the same for any element of the refrigeration cycle. The rate is the result of balance between the compressor and the expansion valve's opening. Together with the heat conservation equations for the lumped heat exchanger, the complete set of equations is developed.

Figure 3 shows the diagram of the components of the simulation and its meaning in the PH Diagram.

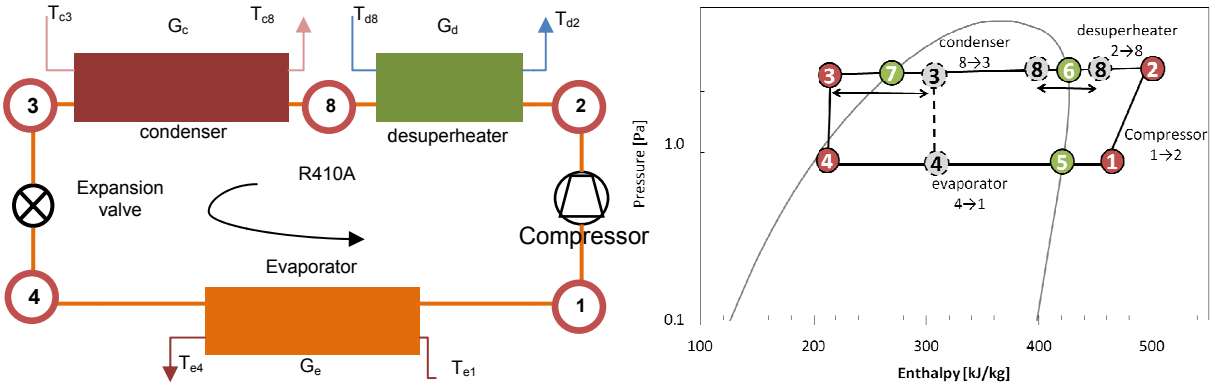

Figure 1 Simulation Components in PH Diagram

Gnielinski's correlation was used for the desuperheater heat exchanger while Shah and Kandlikar's correlations were used for the condensation and evaporation processes. Area restrictions are placed to determine appropriate boundaries of each zone. In order to achieve general convergence, the mass content is calculated for each heat exchanger and for the compressor. The mass inside the expansion valve is very difficult to determine so it is assumed to be zero. As a result, an approximate constant volume that accounts for the expansion valve and the piping of the system is included.

2.3 Boundaries of the problem

Although there are certain variables whose limits cannot be determined, specifically the pressures (P1 and P2) and temperatures T1 and T3 have clear identifiable limits according to the second law of thermodynamics.

The lowest boundary for P1 is theoretically, vacuum. The highest boundary is the pressure at which the refrigerant is boiling at the same temperature as the ground inlet temperature Te1. As the cycle cannot be supercritical, for P2 the highest theoretical limit is the critical pressure of the refrigerant. The lowest limit is the pressure at which the refrigerant is condensing at the same temperature as the highest one from the desuperheater and space heating inlet temperature; which usually will be the space heating unless there is assisted domestic hot water preheating.

Finally, for the inlet temperature to the compressor T1, the minimum temperature is the saturated temperature at the minimum pressure P1. The maximum temperature is equal to the inlet temperature Te1. Figure 2 shows the situation for P1 and P2

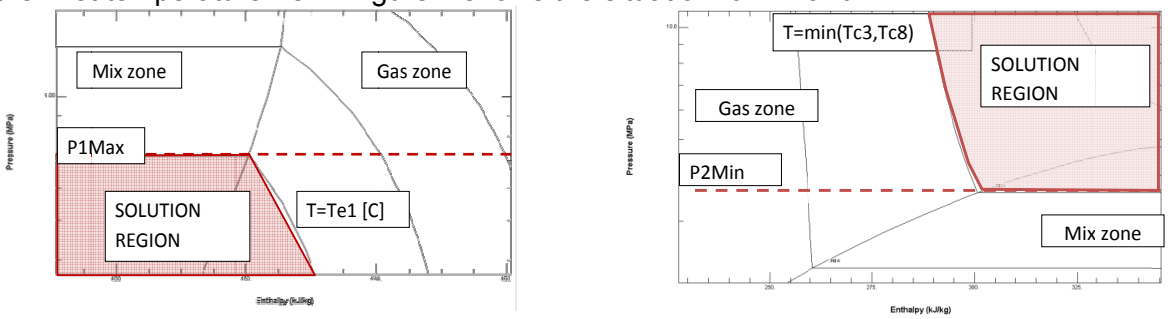

Figure 2, P1 and P2 Boundary conditions

2.4 Component Modeling

2.4.1 Compressor

The compressor is modeled as an adiabatic, isentropic process. In this sense, the work can be defined by the following basic equation

$$w_{id} = \frac{\kappa}{\kappa - 1}\frac{P_1}{\rho_1}\left(\left(\frac{P_2}{P1}\right)^{\frac{\kappa-1}{\kappa}} - 1\right) = \frac{\kappa}{\kappa - 1}P_1 v_1\left(\left(\frac{P_2}{P1}\right)^{\frac{\kappa-1}{\kappa}} - 1\right) \quad (1)$$

Where the real power can be calculated from the mechanical efficiency:

$$W_c = \dot{m}\frac{w_{id}}{\eta_{mech}} \quad (2)$$

For the mass flow rate we have the following relationships.

$$V_f = v_{SW} \cdot freq \quad (3)$$

$$\dot{m} = \eta_v V_f \rho_1 \quad (4)$$

$$\eta_v = 1 + \frac{V_c}{V_{sw}} - \frac{V_c}{V_{sw}}\left(\frac{P_2}{P_1}\right)^{\frac{1}{\kappa}} \quad (5)$$

Where (6)

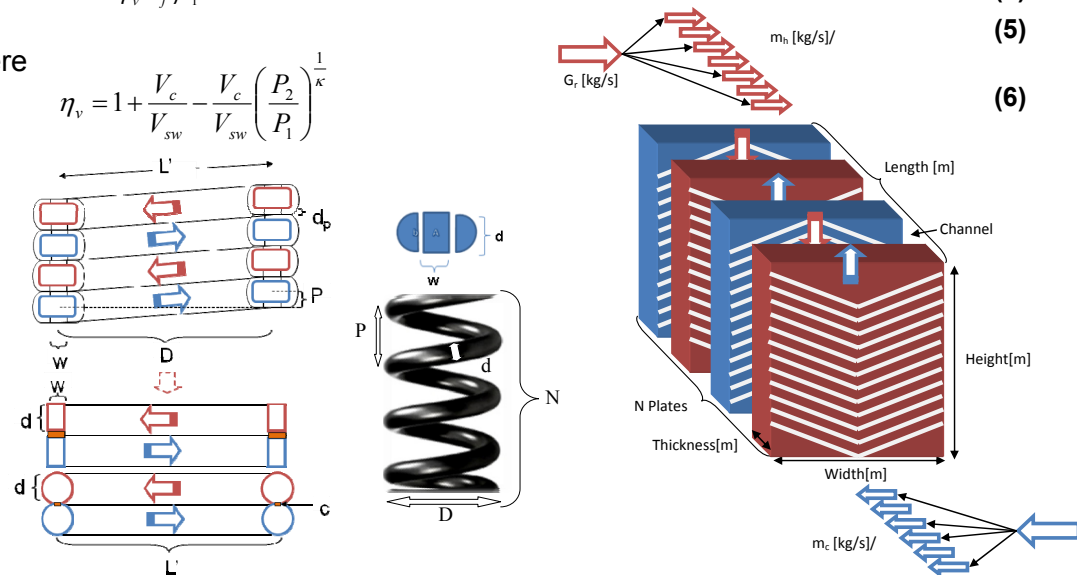

Figure 3 Geometrical parameters of desuperheater and Plate type heat Exchangers

2.4.2 Desuperheater

The development of the desuperheater model and the other heat exchangers is based on the separation of the geometrical aspects from the heat transfer phenomena. The desuperheater is a horizontal, spiral type desuperheater. Heat transfer area Ad is calculated from equation 7 in which c= πd/3 is the contact surface area.

$$L' = \sqrt{(\pi D)^2 + P^2}$$
$$L = NL'$$
$$Ad = L\left(w + \frac{\pi d}{3}\right) \quad (7)$$

The overall heat transfer coefficient is calculated from the following equations in which Nu_c is the enhancement due to the spiral effect (Schmidt 1967). When the saturation point 6 is reached, Shah's correlation is used.

$$f \approx \frac{1}{-1.8\ln\left[\frac{6.9}{\mathrm{Re}} + \left(\frac{\varepsilon / D_h}{3.7}\right)^{1.11}\right]}^2 \quad (8)$$

$$Nu_g = \frac{(f/8)(\mathrm{Re} - 1000)\,\mathrm{Pr}}{1 + 12.7(f/8)^{0.5}(\mathrm{Pr}^{2/3} - 1)} \quad (9)$$

$$\frac{Nu_c}{Nu_s} = 1 + 3.6\left[1 - \left(\frac{d}{D}\right)\right]\left(\frac{d}{D}\right)^{0.8} \quad \textbf{(10)}$$

2.4.3 Condenser and evaporator

The plate type heat exchangers used for the condenser and evaporator are modeled in the same manner. Figure 3 shows the geometrical analysis of the heat exchanger. Only Shah's correlation is presented for reference.

$$A_T = A_P \times (Ch - 1) \quad \textbf{(11)}$$

$$h_m = \left(1 + \frac{3.8}{\left(\frac{1-x}{x}\right)^{0.8}\left(\frac{P}{P_{crit}}\right)^{0.4}}\right)\left(h_l (1-x)^{0.8}\right) \quad \textbf{(12)}$$

Where h_l is calculated by Dittus Boelter correlation.

2.4.4 Expansion valve

The expansion valve is modeled as an orifice, with a variable mass flow rate dictated by the opening step of the valve. The relationship is the following

$$\dot{m} = \eta_{valve}\rho_{3liq}\left[A\left(\frac{step}{A_{\max}}\right)^2 + B\left(\frac{step}{A_{\max}}\right)\right]\sqrt{C\frac{P_2 - P_1}{\rho_{3liq}}} \quad \textbf{(13)}$$

2.5 Heat Balance Equations

In each heat exchanger, heat balance equations are provided for each zone (liquid, mix and gas).

$$\begin{aligned} Q_d &= Q_{dg} + Q_{dm} = \dot{m}(H_2 - H_8) = CG_d(td_2 - td_8) \\ Q_c &= Q_{cg} + Q_{cm} + Q_{cl} = \dot{m}(H_8 - H_3) = CG_c(tc_8 - tc_3) \\ Q_e &= Q_{eg} + Q_{em} = \dot{m}(H_1 - H_4) = CG_e(te_1 - te_4) \end{aligned} \quad \textbf{(14)}$$

where

$$CG_i = Cp_i \cdot G_i \quad \textbf{(15)}$$

Is the heat capacity of the fluid, and 'i' can be either r for refrigerant, or d, c, or e for desuperheater, condenser or evaporator respectively.

Using the NTU method described from equations 16 to 21 the appropriate heat transfer for each zone can be found. It is important to note that for the case of the desuperheater, the mix zone heat transfer can be zero depending on the output conditions, meaning that the refrigerant is still in gas state when entering the condenser. A similar argument can be applied to the condenser.

$$Qij = \varepsilon_{ij} Qij_{\max} \quad \textbf{(16)}$$

$$\varepsilon_{ij} = \frac{1 - e^{-NTU_{ij}(1-C_{ij})}}{1 - C_{ij}e^{-NTU_{ij}(1-C_{ij})}} \; no\ phase\ change \quad \textbf{(17)}$$

$$\varepsilon_{ij} = 1 - e^{-NTU_{ij}} \; phase\ change$$

$$C_{ij} = \frac{\min(CG_{rj}, CG_i)}{\max(CG_{rj}, CG_i)} \quad \textbf{(18)}$$

$$Qij_{\max} = CG_{i\min}\left(T_2 - T_{d8}\right) \quad \textbf{(19)}$$

$$CG_{i\min} = \min(CG_r, CG_i) \quad \textbf{(20)}$$

$$NTU_{ij} = \frac{U_{ij}A_{ij}}{CG_{i\min}} \quad \textbf{(21)}$$

Where 'j' represents the zone of consideration: g, o or l for gas, mix and liquid zones.

2.6 Refrigeration Charge

The total mass of the system can be determined from the sum of masses on each component. We have for each zone of heat transfer

$$M_{ig} = V_{ig} \cdot \overline{\rho}_{ig} \qquad M_{im} = V_{im} \cdot \overline{\rho}_{im} \qquad M_{il} = V_{il} \cdot \overline{\rho}_{il}$$

While for the gas and liquid zones the average density can be easily calculated, for the mix zone, the approach presented by (Fukushima, Arai and Arai 1977) is used. The mass content is calculated from the void fraction as follows:

$$M_m = V_m(\beta_m \cdot \rho_g + (1-\beta_m)\cdot \rho_l \quad \textbf{(22)}$$

Where the void fraction parameter β_m can be calculated from

$$\beta_m = \frac{v_g}{x_2 - x_1}\left[\frac{x}{v_g - v_l} - \frac{v_l}{(v_g - v_l)^2}\cdot \ln(x\cdot(v_g - v_l) + v_l)\right]_{x_1}^{x_2} \quad \textbf{(23)}$$

and x_2 and x_1 are the inlet and outlet quality respectively.

2.7 Programming Environment

Although many programming suites are appropriate for developing the simulation, Engineering Equation Solver was chosen for several reasons. First, a comparison made between the property tables found in Refprop vs. 8 and EES 6.88 for the enthalpy change showed that the difference was less than 1% therefore by using EES the tradeoff for precision by speed was small, and faster access to the properties of state of the refrigerant was possible, which in other program architectures resulted in extremely slow programs. Second, EES has the possibility of solving the nonlinear mathematical models by the Simultaneous Solving Method as well as the Sequential Module method. Third, it has important tools regarding the completeness of equations, unit check, parametric analysis, optimization techniques and it has been tuned up for thermodynamic applications.

2.8 Convergence Strategy

The simulation closure is based on mass flow rate convergence between expansion valve and compressor models. The mass flow rate difference can be described by the function g:

- $\dot{m}_1$ =compressor(parameters, P1, P2)
- $\dot{m}_2$=expansion Valve(parameters, P1, P2)

and

$$g(P1, P2) = \dot{m}_1 - \dot{m}_2 \quad \textbf{(24)}$$

Although it is not clear what is the shape of the function '*g'* in the P1-P2 space, it will be argued that for one pressure P1 and an initial set of conditions, there is only one P2 that satisfies '*g'=0.* Therefore, '*g'=0* cuts the plane P1-P2 in two regions (positive and negative), at least for the region of interest delimited by maximum and minimum allowable pressures. To facilitate the visualization of the relationship, on the figure bellow at the left, the mass flow rate was plotted against P2, for certain values of P1. The family of curves is then compared

for the compressor and expansion valve. The red dotted line identifies the curve where g=0. The red shaded area limits the boundary conditions setup by the inlet parameters.

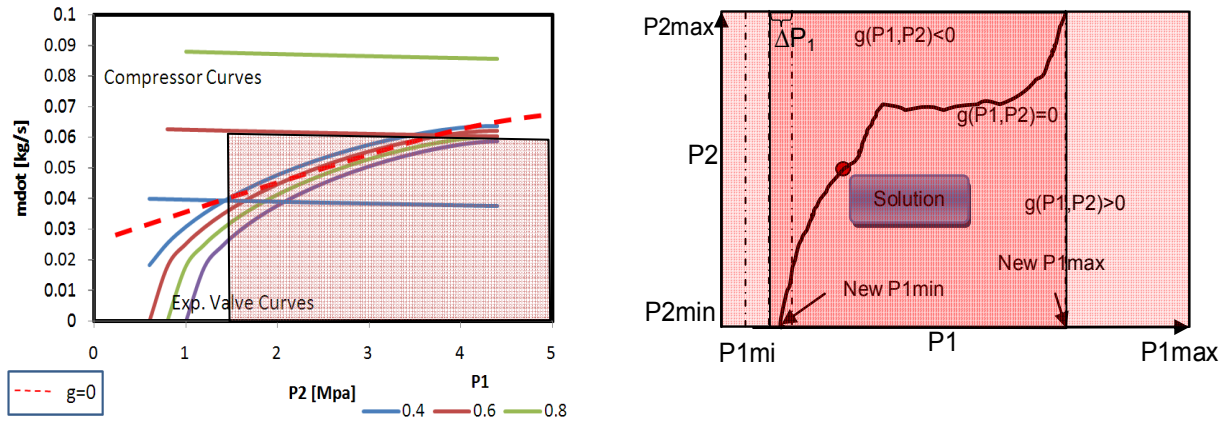

Figure 4 (Left) Mass flow rate vs. Pressure two for certain values of P1, (right) Refinement of P1 boundary conditions

From the above figure at the right, it can be seen that the line plotted by '*g*' can also directly restrict the range of acceptable values for P1, therefore refining the area of interest. For P1 < P1mi, there is no root for '*g*' in the shaded region. The same occurs for pressures above the New P1Max. To find the new boundaries for P1 we divide the segment in equal parts ΔP1 and we evaluate g for the maximum and minimum values of P2 as shown in the above figure at the right. Then, the target area is refined.

The final condition of convergence is set making use of the refrigerant charge. The final solution is obtained when the calculated mass charge agrees with input charge.

2.8.1 Ridders algorithm

As an analytical equation that describes our function 'g' is not available, Ridders Algorithm *(William, et al. 2007)* is used. Although not being the fastest, it guarantees convergence when the boundaries are laid out. The equation for Ridders Implementation which uses the last three values of 'g' is the following:

$$P_2^{\,4} = P_2^{\,3} + \left(P_2^{\,3} - P_2^{\,1}\right)\frac{sign\left[g(P_1,P_2^{\,1}) - g(P_1,P_2^{\,2})\right]g(P_1,P_2^{\,3})}{\sqrt{g(P_1,P_2^{\,3})^2 - g(P_1,P_2^{\,1})\,g(P_1,P_2^{\,2})}} \qquad (25)$$

2.8.2 Nelder-Mead method

Until this point, from an initial P1 which is within the boundary conditions its pair P2 has been found such that '*g*'=0. In addition, T1 should be selected so that the convergence conditions are met for the selected point. Therefore, the problem is reduced on selecting the best P1 and T1 in the P-T plane. A function error is defined which shows the distance between initial and final points. It can be defined as

$$error = \sqrt{(T1 - T1')^2 + (H1 - H1')^2 + (M - M')^2} \qquad (26)$$

in which T1 and T1' and H1 and H1' represents the initial and final temperature and the initial and final enthalpies of point 1 respectively; and M and M' represents the difference between the input charge *M* and the calculated charge *M'*. The final solution of the cycle will be obtained for the pressure P1 and T1 that minimizes the error function of equation 26. The Nelder-Mead method (Samuel 1992) was selected as there is no analytical equation to apply other techniques involving the derivate of 'g'. Also, this algorithm guarantees finding of a

minimum point, and can be tracked down within the boundary limits at every step. To test the simulation, a thorough experiment was conducted, which will be explained in the following chapter.

3 EXPERIMENTAL SETUP

A compact GSHP with coil type desuperheater was developed by SUNPOT Co. Ltd. and tested in Hokkaido University Human Environmental System's Laboratory.

An inverter controlled compressor is used to provide variable speed to cope with variable load characteristics. Plate type heat exchangers operated in counterflow arrangement are used both for the condenser and evaporator. The expansion process is achieved via an electronically step controlled expansion valve. For the desuperheater, a counterflow parallel coil type heat exchanger is used. The main components of the cycle are shown in Figure 1

3.1 Test Station and Connection

The test station simulates primary and secondary sides of the heat pump by the use of brine tanks controlled by variable speed pumps. The connecting pipes to the GSHP use PID controllers to provide a steady volumetric flow rate. PID controllers also manage the heat exchange between the primary and secondary sides to maintain a constant temperature condition for the GSHP. For the desuperheater, a constant temperature chamber and a variable speed pump controls the inlet temperature and volumetric flow rate to the desuperheater. The general setup of the experiment is shown in figure 5.

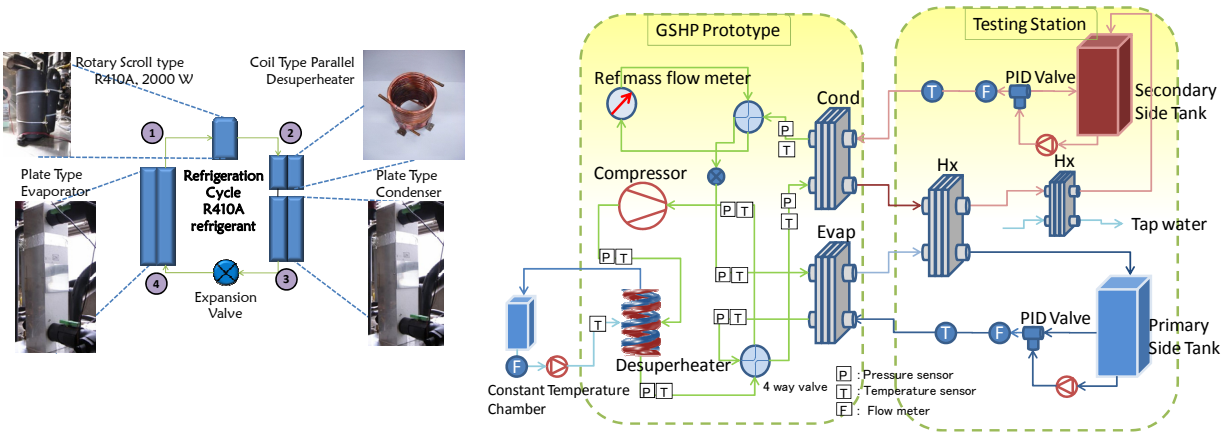

Figure 5 Compact GSHP with Desuperheater (left) and Test Station (right)

3.2 Testing conditions:

The experimentation scenarios were divided according to the following target environmental conditions:

Table 1 Experimental Conditions

Td2	Tc8	Td8	Te1	Freq	Step
Domestic hot water outlet: 65˚C (Constant)	Space heating: 35 and 45 ˚C	Tap water inlet temperature: 5, 17, 30 ˚C	T_{e1}: Ground Output temperature: -5, 0, 5 ˚C	Compressor Frequency: 30, 45, 60, 75, 90 Hz	Expansion Valve opening: range according to limiting conditions

3.3 Experimental Results

The available operation range shows the maximum and minimum performance that can be obtained for each set of conditions. Data is only shown for space heating and domestic hot water.

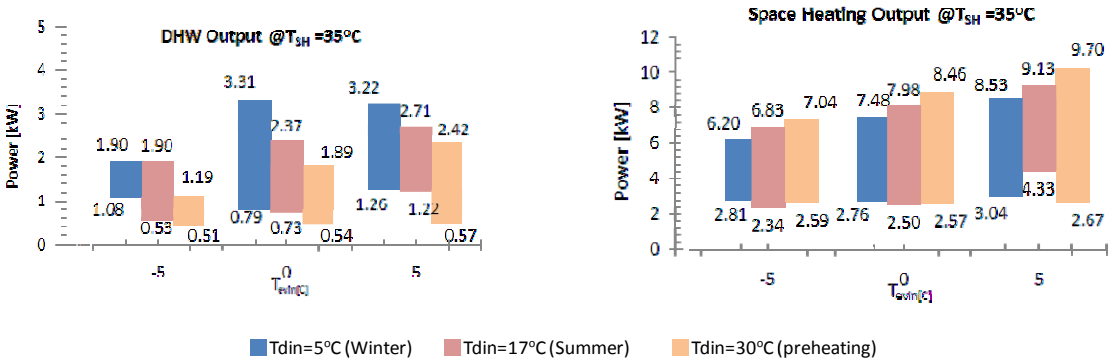

Figure 6 Experimental operation ranges

4 RESULTS AND DISCUSSION

Examining the experimental results, it is seen there is a minimum heating output of 6.20 kW in the coldest environmental conditions for winter. Therefore, the heat pump can cope with the thermal demand for a medium size low energy house (220 m^2). The information collected from the experimental results was used for determining the parameters used for the simulation. The method of least squares was used for fitting of non geometrical parameters.

To test the algorithm convergence, three different initial points inside the boundary conditions were selected. The solution was obtained from the three cases with less than 1% of difference between each, showing the completeness of the system. Simulation was completed in 10 minutes average. The number of iterations versus the distance function and the heat balance of the final result are shown in the following figure.

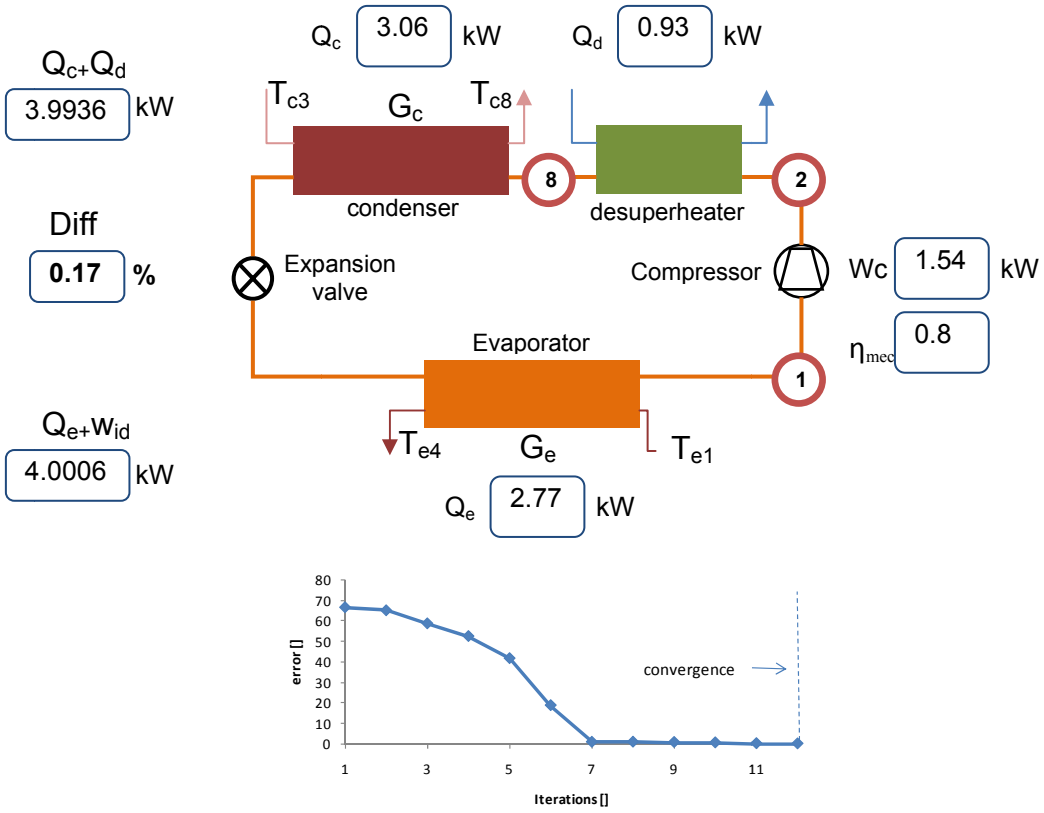

Figure 7 Heat Balance and Iteration towards answer for case examined

Finally, the experimental pool of 118 experimental inlet conditions was simulated. The results show relatively good agreement for each of the heat exchangers. Nevertheless the sum of difference is rather noticeable when examining the COP. This phenomenon can be examined in figure 9.

Additionally, the simulation tool can be used for design. For a particular operation condition, the optimum expansion valve opening was determined in order to maximize the COP. For this step, a parametric analysis on the number of plates for the condenser and evaporator heat exchangers was performed. It was shown that increasing the number of plates over 40 the contribution of area to the heat exchange is small.

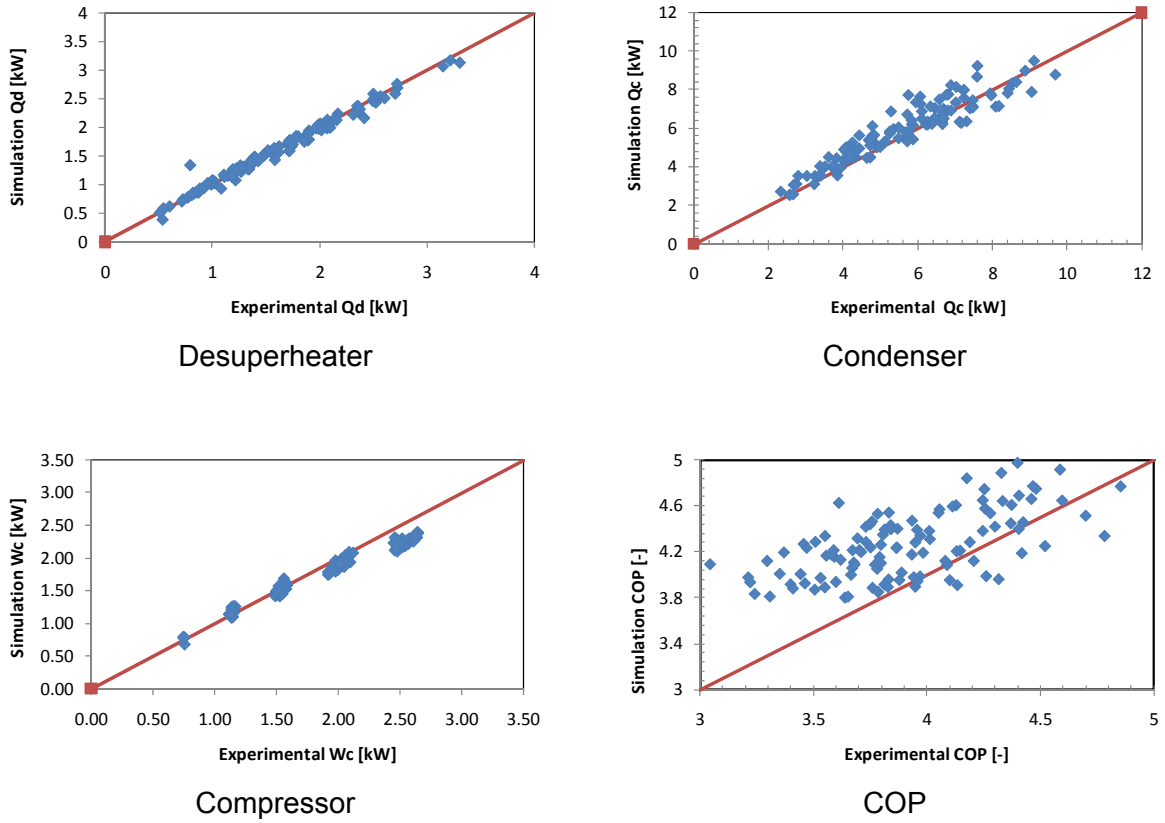

Figure 8 Element Simulation versus experimental results

Table 2 Study case for COP maximization

inlet	te1[℃]	Ge [L/min]	td8 [℃]	Gd [L/min]	tc3 [℃]	Gc [L/min]	Freq [Hz]	Step
	4.8	24.5	17.7	0.6	28.8	16	75	340

Simulation	Wc [kW]	Gr [kg/min	p1[MPA]	t1[℃]	te4 [℃]	td2 [℃]	tc8 [℃]
	1.92	3.01	0.57	-10.3	0.30	65.64	36.29

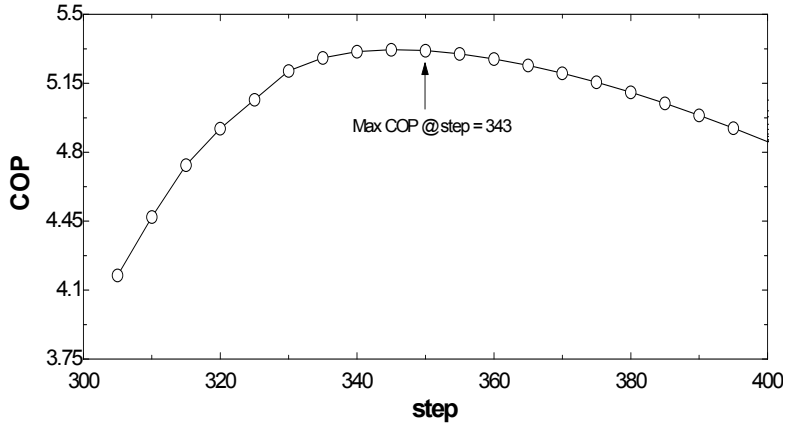

Figure 9 Simulation Result of COP vs Step for the GSHP with desuperheater

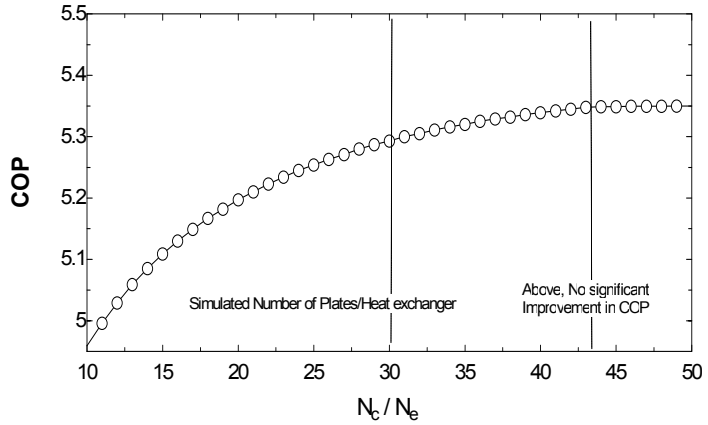

Figure 10 Number of plates versus COP

5 CONCLUSIONS

A compact GSHP with desuperheater was constructed and tested, showing to cope with the thermal heating demand for a low energy house in the northern Japanese environmental conditions. The mapping results show how partial demand is achievable for each different environmental condition selected. As low as 1 kW and as much as 3 kW could be extracted by the use of the desuperheater.

A refrigerant cycle simulation has been constructed which is based on physical parameters of the components and thermodynamic properties. Convergence algorithms are applied. A mathematical scheme and mathematical minimization techniques are applied so as to reduce iterations.

The simulation program was used to find the step opening for the expansion valve that maximizes the COP of the system for a particular case. Parametric analysis on the number of plates for the condenser and evaporator showed that above 40 plates the tradeoff between area and heat exchanger gained was small, because the heat exchangers are approximating the pinch state.

6 REFERENCES

Swardt, C. A., and J. P. Meyer. "A performance comparison between an air-source and a ground-source reversible heat pump." International Journal of Energy Research 2001 Vol 25 p. 899-910.

Ding, Guo-liang. "Recent developments in simulation techniques for vapour-compression refrigeration systems." *International Journal of Refrigeration* 2007 Vol 30, p. 1119-1133.

Katsura, Takao, Katsunori Nagano, Shogo Hori, and Hikaru Umezawa. "Performance Test and Feasibility Study of Integrated Ground Source Heat Pump for Low Energy House." 9th International IEA Heat Pump Conference. Zürich, Switzerland

Samuel, Wong. Computational Methods in Physics and Engineering. Prentice-Hall Inc, New Jersey

Schmidt, E.F. "Wärmeübergang und Druckverlust in Rohrschlangen." Chemical Ing. Technik vol 39, no. 13 p. 781-789.

William, Press, Saul Teukolsky, William Vetterling, and Brian Flannery. Numerical Recipes. Cambridge University Press, New York

Belman JM, Navarro-Esbri, J., Ginestar D., Steady state model of a avariable speed vapor compression system using R134a as working fluid" International Journal of Energy Research, 2009

ACKNOWLEDGEMENT

The author is grateful to Dr. Katsura Takao and MC Umezawa Hikaru for fruitful discussions reflected in the paper, as well as Associate Professor Harada from Sustainable Resource Engineering Department from Hokkaido University for introducing several modeling techniques. The collaboration of Sunpot Co. Ltd. and its heat pump team is greatly appreciated. The experimental setup and analysis wouldn't have been possible without the close collaboration of MC Morimoto Masahiro.

NOMENCLATURE

Thermodynamic properties

Symbol	Meaning	Units
t	Temperature	K
p	Pressure	MPa
ρ	Density	kg/m^3
H	Enthalpy	kJ/kg
S	Entropy	kJ/kg-K
c	Specific heat	kJ/kg-K
x	Quality	-

Other sub indexes

letter	Meaning
d	Desuperheater
c	Condenser
s	Subcooler
e	evaporator
r	Refrigerant
w	Water
h	Hot
c	cold
ε	Height of roughness
t	transversal

Transportation Properties and Special Numbers

Symbol	Meaning	Units
λ	Thermal conductivity	kW/m-K
μ	Viscosity	μPa-s
κ	Adiabatic index	-
η	Efficiency	-
G	Mass Flow	kg/s
Re	Reynolds Number	-
Nu	Nusselt Number	-
Pr	Prandtl Number	-
F	Fanning Factor	-